

TABLE OF CONTENTS

	Page
Acknowledgement	iii
Abstract (English)	v
Abstract (Thai)	ix
List of tables	xxvii
List of figures	xxx
Abbreviations and symbols	xxxviii
Chapter 1 Introduction	
1.1 Statement and significance of the problem	1
1.2 Objective	4
1.3 Scope of study	4
1.4 Literature reviews	5
1.4.1. Green fluorescent protein (GFP)	5
1.4.1.1. Introduction	5
A. Historical perspective	5
B. Chromophore formation	9
1.4.1.2. Applications of GFP	11
A. Fusion tags	11
B. The reporter gene	12
C. Fluorescence resonance energy transfer (FRET)	13

D. Photobleaching	14
E. Protein-Protein interaction	15
F. Other applications	16
1.4.2. Calcitonin	17
1.4.2.1. Introduction	17
1.4.2.2. Physiologic roles of calcitonin	20
1.4.2.3. Indications	21
A. Osteoporosis	22
B. Paget's disease	22
C. Analgesic effect	23
1.4.2.4. Pharmaceutical sCT formulations	23
1.4.2.5. Calcitonin receptor (CTR) and cell signaling	24
1.4.3. Cell penetrating peptides (CPPs)	25
1.4.3.1. Introduction	25
1.4.3.2. Mechanism of translocation	27
1.4.3.3. Applications	32
A. The targeted and enhanced delivery	32
B. Protein and peptide delivery	33
C. Antisense nucleotides delivery	34
D. Peptide nucleic acids (PNAs) delivery	35
E. siRNA delivery	35

F. Liposome delivery	36
G. Plasmid delivery	36
1.4.3.4. Tat peptide	39
A. Introduction	39
B. Tat and cell surface interactions	40
C. Possible mechanisms of internalisation	46
1.4.4. Poliovirus	50
1.4.4.1. General introduction	50
1.4.4.2. The structure of poliovirus	52
1.4.4.3. Cellular life cycle	54
A. Cell entry	54
B. Polyprotein translation and proteolytic processing	56
C. RNA replication	57
1.4.4.4. Poliovirus receptor (PVR, CD155) and pathogenesis	60
1.4.4.5. Interaction of poliovirus receptor to poliovirus	64
1.4.4.6. Application of poliovirus capsid proteins	67
A. Drug design	67
B. Ligand-receptor mediated drug targeting	69
1.4.5. Protein and peptide delivery systems	70

1.4.5.1. Barriers of protein and peptide delivery	70
A. Physical barriers: size, charge and solubility constraints	70
B. Enzymatic barriers	70
1.4.5.2. Strategy for peptide delivery	74
A. Chemical modification	74
B. Protease inhibitors co-administration	76
C. Absorption enhancers	77
D. Formulation vehicles	79
1. Emulsions	79
2. Hydrogels	80
3. Polymeric Particulate Systems	81
4. Nanovesicles	81
E. Cell penetrating peptides (CPPs)	82
1.4.6. Protein expression	82
1.4.6.1. Fundamental techniques	82
A. Polymerase chain reaction (PCR)	82
B. Agarose gel electrophoresis	87
C. SDS-PAGE	88
D. Western blot analysis	90
1.4.6.2. Generation of expression plasmids	91
A. Multi-parallel molecular cloning strategies	91
B. Choice of tag	93

1.4.6.3. Expression system	95
A. <i>Escherichia coli</i> -mediated protein expression	95
B. Baculovirus-mediated insect cell protein expression	96
C. Other expression systems	97
1.4.6.4. Protein purification	99
 Chapter 2 Materials and methods	
2.1. Materials and equipments	100
2.1.1. Chemicals	100
2.1.2. Animals	102
2.1.3. Cell lines, bacterial cultures and plasmids	102
2.1.4. Equipments	102
2.2 Methods	105
Part 1 : Construction of GFP, Tat/GFP, VP/GFP and VP/Tat/GFP fusion proteins expression plasmid	106
1.1. Primer design	106
1.2. Amplification of genes encoding GFP or fusion protein	107
1.3. Linearization of pET28a(+) expression vector and PCR fragment digestion	107
1.4. Ligation reaction	108

Part 2 : Expression and purification of GFP, Tat/GFP, VP/GFP and VP/Tat/GFP fusion protein	109
2.1. Transformation	109
2.2. Protein expression	110
2.3. Purification and analysis	110
2.3.1. Ni-NTA purification	110
2.3.2. SDS-PAGE and western blot analysis	111
2.3.3. Protein concentration determination by Bradford method	112
2.3.4. Fluorescent intensity measurement	113
Part 3 : Cellular uptake of GFP, Tat/GFP, VP/GFP and VP/Tat/GFP fusion proteins	113
3.1. Cell culture	113
3.2. Cellular uptake study	113
Part 4 : Cellular uptake efficiency enhancement strategy	114
4.1. Entrapment in nanovesicles	114

4.1.1. Preparation of the empty nanovesicles (liposomes/niosomes)	115
4.1.2. Physical properties determination of nanovesicular formulations	115
A. Mean particle sizes and zeta potential	116
B. Entrapment efficiency of Tat-GFP loaded in nanovesicles	116
C. Deformability index (DI) determination	117
4.1.3. Cellular uptake study of Tat- GFP loaded nanovesicles	117
4.1.4. Chemical stability determination of Tat-GFP loaded nanovesicles	117
4.1.5. Cytotoxicity of nanovesicular formulations by the SRB assay	118
4.1.6. Development of low toxic elastic anionic niosomes	118
4.1.7. Transdermal absorption study	119

A. Preparation of rat skin	119
B. Transdermal absorption experiment	120
4.2. Tat/GFP, VP/GFP and VP/Tat/GFP mixture	121
4.2.1. Evaluation of simple mixing method as cargoes transport strategy	121
A. Cellular uptake study	121
B. Transepithelial study	121
C. Transdermal delivery through rat skin	122
4.2.2. Tat/GFP, VP/GFP and VP/Tat/GFP mixture preparation	122
4.2.3. Cellular uptake study of Tat/GFP, VP/GFP and VP/Tat/GFP mixture	123
Part 5 : <i>In vitro</i> calcitonin activity study of Tat/sCT, VP/sCT and VP/Tat/sCT mixture	123
5.1. Mixture preparation	123
5.2. Physical properties of mixture	123
5.2.1. Size and zeta potential determination	124

5.2.2. Differential scanning calorimetry (DSC)	124
5.2.3. Fourier transform infrared spectroscopy (FT-IR)	124
5.3. <i>In vitro</i> calcitonin activity experiment	124
5.4. Determination of poliovirus receptor (PVR) expression	125
Part 6 : <i>In vivo</i> calcitonin activity of Tat/sCT, VP/sCT and VP/Tat/sCT mixture	126
6.1. Animals	126
6.2. Subcutaneous administration of sCT	126
6.3. Oral administration of Tat/sCT, VP/sCT and VP/Tat/sCT mixture	126
6.4. Transdermal absorption of sCT and Tat/sCT at 1:1 molar ratio	127
6.5. Chemical stability of sCT and Tat/sCT mixture	127

Chapter 3 Results and discussion

Part 1 : Construction of GFP, Tat/GFP, VP/GFP and VP/Tat/GFP fusion protein expression plasmid	129
--	-----

1.1. Amplification of genes encoding GFP, Tat/GFP, VP/GFP and VP/Tat/GFP	129
1.2. Construction of GFP, Tat/GFP, VP/GFP and VP/Tat/GFP fusion protein expression vectors	131
Part 2 : Expression and purification of GFP, Tat/GFP, VP/GFP and VP/Tat/GFP fusion protein	134
2.1. Transformation of expression vectors and colony screening	134
2.2. Protein expression and purification	136
2.2.1. Target protein verification for expression level and solubility	136
2.3. Analysis of purified proteins	136
Part 3 : Cellular uptake of GFP, Tat/GFP, VP/GFP and VP/Tat/GFP fusion protein	140
Part 4 : Cellular uptake efficiency enhancement strategy	145
4.1. Entrapment in nanovesicles	146
4.1.1. Preparation and physical properties determination of nanovesicular formulations (liposomes/niosomes)	146
A. Mean particle sizes and zeta potential	146

B. Entrapment efficiency of Tat-GFP loaded in nanovesicles	147
C. Deformability index (DI) determination	150
4.1.2. Cellular uptake and cytotoxicity of Tat-GFP loaded nanovesicles	151
4.1.3. Chemical stability determination of Tat-GFP loaded nanovesicles	154
4.1.4. Development of low toxic elastic anionic niosomes	156
4.1.5. Cellular uptake and cytotoxicity	160
4.1.6. Transdermal absorption study	161
4.2. Tat/GFP, VP/GFP and VP/Tat/GFP mixture	164
4.2.1. Evaluation of simple mixing method as cargoes transport strategy	164
4.2.2. Cellular uptake study of Tat/GFP, VP/GFP and VP/Tat/GFP mixture	169
Part 5 : <i>In vitro</i> calcitonin activity of Tat/sCT, VP/sCT and VP/Tat/sCT mixture	170
5.1. Physical properties of the mixture	170
5.1.1. Sizes and zeta potential determination	170

5.1.2. Differential scanning calorimetry (DSC) and Fourier transform infrared spectroscopy (FT-IR)	172
5.2. <i>In vitro</i> calcitonin activity experiment	181
Part 6 : <i>In vivo</i> calcitonin activity of Tat/sCT, VP/sCT and VP/Tat/sCT mixtures	182
6.1. Subcutaneous administration of sCT	182
6.2. Oral administration of Tat/sCT, VP/sCT and VP/Tat/sCT mixtures	184
6.3. Transdermal absorption of sCT and Tat/sCT at 1:1 molar ratio	186
6.4. Chemical stability of sCT and Tat/sCT mixture	190
Chapter 4 Conclusion	
Part 1 : Construction of GFP, Tat/GFP, VP/GFP and VP/Tat/GFP fusion protein expression plasmid	192
Part 2 : Expression and purification of GFP, Tat/GFP, VP/GFP and VP/Tat/GFP fusion protein	192
Part 3 : Cellular uptake of GFP, Tat/GFP, VP/GFP	193
Part 4 : Cellular uptake efficiency enhancement strategy	194
4.1. Entrapment in nanovesicles	194

4.2. Tat/GFP, VP/GFP and VP/Tat/GFP mixture	195
Part 5 : <i>In vitro</i> calcitonin activity of Tat/sCT, VP/sCT and VP/Tat/sCT mixture	196
Part 6 : <i>In vivo</i> calcitonin activity of Tat/sCT, VP/sCT and VP/Tat/sCT mixture	197
References	200
Appendices	234
Appendix A Chemical and physical properties of substances used in this study	235
Appendix B Plasmid map	242
Appendix C Formulation of buffer and solution used in this study	244
Appendix D Amino acids sequence of GFPmut2	246
Appendix E Calculation of nanovesicle compositions	247
Curriculum vitae	249

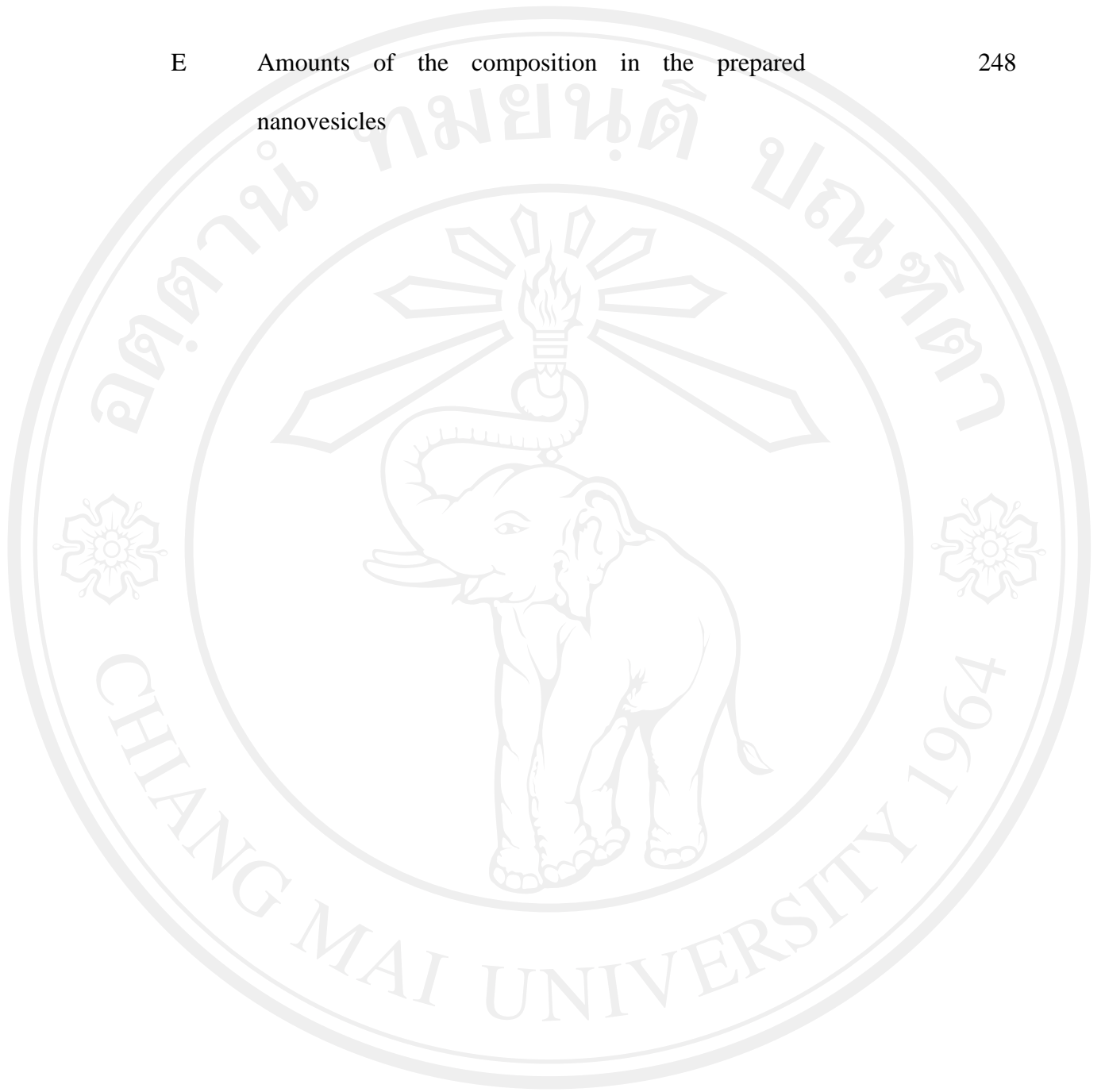
LIST OF TABLES

Table		Page
1	Nucleotide and amino acid sequence of GFP of wild-type <i>Aequorea victoria</i>	8
2	Selection of the commonly used CPPs	27
3a	Bond specificities of secreted peptidases	72
3b	Intestinal brush-border membrane-bound peptidases	72
4	Comparison of commonly used tags for purification and expression enhancement	94
5	The amount of each component (μ l) in PCR reaction	108
6	Vesicular sizes (nm) and zeta potential (mV) of the blank and Tat-GFP loaded nanovesicles	148
7	Entrapment efficiency of Tat-GFP fusion protein in various nanovesicular formulations	149
8	Deformability index (DI) and the DI ratios of the blank nanovesicles	151
9	Cellular uptake of Tat-GFP fusion protein and cell viability of HT-29 cells after incubated with various nanovesicular formulations	153
10	Vesicle sizes, zeta potential and DI of blank elastic and non-elastic anionic niosomes containing ethanol, NaC or NaDC at various concentrations	157

11	Entrapment efficiencies of Tat-GFP loaded in different elastic vesicular formulations	159
12	Cellular uptake and cytotoxicity of Tat-GFP loaded in elastic and non-elastic niosomes in HT-29 and KB cells	162
13	The cumulative amounts ($\mu\text{g}/\text{cm}^2$) and fluxes ($\mu\text{g}/\text{cm}^2\text{h}$) of GFP and Tat-GFP from various systems in SC, VED and receiver compartment following transdermal absorption across excised rat skin at 6 hours by vertical Franz diffusion cells	163
14	Transdermal absorption across excised rat skin of GFP, Tat-GFP fusion protein and Tat/GFP mixture at 6 hours in stratum corneum (SC), viable epidermis and dermis (VED) and receiver compartment of vertical Franz diffusion cells	168
15	Particle sizes (nm) and zeta potential (mV) of sCT, Tat, VP and Tat/VP/sCT mixtures at various molar ratios	174
16	Percentage remaining of sCT in sCT solution and Tat/sCT mixture after 1 month storage at different temperatures	191
D	Amino acid sequences of GFPmut2 (237 amino acids)	247

E Amounts of the composition in the prepared
nanovesicles

248



ลิขสิทธิ์มหาวิทยาลัยเชียงใหม่
Copyright© by Chiang Mai University
All rights reserved

LIST OF FIGURES

Figure		Page
1	Bioluminescence in <i>Aequorea victoria</i>	7
2	Solid-state structures of GFP, the chromophore is located in the center of the 11-sheet β -barrel	9
3	The amino acid sequences of salmon calcitonin	18
4	Proposed mechanisms of cellular delivery of cargos mediated by cell penetrating peptides (CPP)	29
5	Proposed models for MPG-mediated membrane translocation of nucleic acids (A) and model of Pep-1-mediated transfer of proteins through lipid bilayers (B)	31
6	Utility of protein transduction technology	38
7	Genomic organization and proteolytic processing of poliovirus	53
8	Hypothesis for poliovirus transport through the axon. Human poliovirus receptor (hPVR)-mediated endocytosis occurs at synapses	64
9	The mature structure of human PV receptor (hCD155)	65
10	The footprint of the CD155 on the PV surface	66

11	Structures of “carrier” molecules used for enhancing oral bioavailability of protein and peptide drugs	80
12	Schematic drawing of the PCR cycle	90
13	Agarose electrophoresis of (A) pET28a(+) digested with HpaI (lane 1), pET28a(+)GFP digested with HpaI (lane 2), pET28a(+)GFP-Tat digested with HpaI	90
14	Scope of the study	105
15	Experimental set-up of Franz diffusion cell apparatus	121
16	PCR product of GFP (A) and GFP-Tat (B)	130
17	PCR product of VP-GFP	130
18	Agarose electrophoresis of (A) 1 kb DNA ladder (lane 1), linearized pET28a(+) (lane 2), digested GFP (lane 3) and digested GFP-Tat (lane 4) (B) 1 kb DNA ladder (lane 1), linearized pET28a(+) (lane 2) and digested Tat-GFP	131
19	Agarose electrophoresis of linearized pET28a(+) (lane 1), digested VP-GFP (lane 2) and digested Tat-GFP-VP (lane 3)	132
20	Agarose electrophoresis of ligation products (A) pET28a(+)GFP (lane 1; 6059 bp), pET28a(+)GFP-Tat (lane 2; 6086 bp) and 1 kb DNA ladder. (B) 1 kb DNA ladder (lane 1), pET28a(+)Tat-GFP (lane 2; 6086 bp) and pET28a(+) (lane 3; 5369 bp)	132

21	Agarose electrophoresis of ligation products (A) VC 1 kb DNA ladder (lane 1) and pET28a(+)VP-GFP (lane 2; 6110 bp) (B) VC 1 kb DNA ladder (lane 1) and pET28a(+)Tat-GFP-VP (lane 2; 6137 bp)	133
22	Agarose electrophoresis of (A) pET28a(+) digested with HpaI (lane 1), pET28a(+)GFP digested with HpaI (lane 2), pET28a(+)GFP-Tat digested	133
23	<i>E. coli</i> DH5 α transformed with pET28a(+) (A and G), pET28a(+)GFP (B and H), pET28a(+)GFP-Tat (C and I), pET28a(+)Tat-GFP (D and J), pET28a(+)VP-GFP (E and K) and pET28a(+)Tat-GFP-VP (F and L). A-F and G-L were captured under transmission light and fluorescent filter, respectively	134
24	SDS-PAGE analysis of the expressed proteins from non-transformed <i>E. coli</i> BL21 (DE3) (lane 2), <i>E. coli</i> BL21 (DE3) transformed with pET28a(+) (lane 3), <i>E. coli</i> BL21 (DE3) transformed with pET28a(+)GFP (lane 4, 6 and 8) and <i>E. coli</i> BL21 (DE3) transformed with pET28a(+)GFP-Tat (lane 5, 7 and 9). Lanes 2-5 were TCP fraction. Lanes 6-7 were soluble cytoplasmic fractions. Lanes 8-9 were insoluble cytoplasmic fractions	137

- 25 SDS-PAGE analysis of GFP (A) and GFP-Tat (B) 138
 expression after IPTG induction at final concentration 0.1 mM (lane 2), 0.2 mM (lane 3), 0.4 mM (lane 4) and 1 mM (lane 5) for 3 hr
- 26 SDS-PAGE analysis of GFP (A) and GFP-Tat (B) 138
 expression after IPTG induction at final concentration 0.1 mM for 1 hr (lane 2), 2 hr (lane 3), 3 hr (lane 4), 4 hr (lane 5) and 5 hr (lane 6)
- 27 (A) Analysis of the purified GFP (lane 2; ~28 kDa) 139
 and GFP-Tat (lane 3; ~30 kDa) and Tat-GFP (lane 4; ~30 kDa) by 12% SDS-PAGE (B) Purified Tat-GFP (lane 1; ~30 kDa), VP-GFP (lane 2; ~30 kDa) and Tat-GFP-VP (lane 3; ~32 kDa) resolved in SDS-PAGE
- 28 Western blot analysis using anti-penta-His-HRP 139
 conjugate antibody. M : molecular weight markers, G : GFP, G-T : GFP-Tat fusion protein, T-G : Tat-GFP fusion protein
- 29 Fluorescent intensity at various concentrations of 140
 GFP, GFP-Tat, Tat-GFP, VP-GFP and Tat-GFP-VP fusion protein

30	Cellular uptake efficiency represented as percentage of protein detected in HT-29 and KB cells after 1 hour incubation with GFP or Tat/GFP fusion proteins at 1 μ M	141
31	Cellular uptake efficiency of GFP and Tat/GFP fusion proteins in HT-29 cell lines as fluorescent intensity units (rfu) after incubation for 1 hour with various concentrations of GFP, GFP-Tat and Tat-GFP fusion proteins	142
32	The effect of incubation on cellular uptake of GFP and Tat/GFP fusion proteins in HT-29 cell lines. The concentration of all samples was 1 μ M	142
33	CLSM pattern from uptake study of N-terminal 6XHis GFP, GFP-Tat and Tat-GFP	143
34	Cellular uptake efficiency represented as percentage of protein detected in HT-29 and KB cells after 1 hour incubation with GFP or Tat/VP/GFP fusion proteins at 1 μ M	145
35	The percentages of fluorescent signal remaining in comparing to at initial of Tat-GFP loaded in elastic and non-elastic anionic niosomes and the non-loaded Tat-GFP when stored at 30 \pm 2 $^{\circ}$ C for 3 months	155

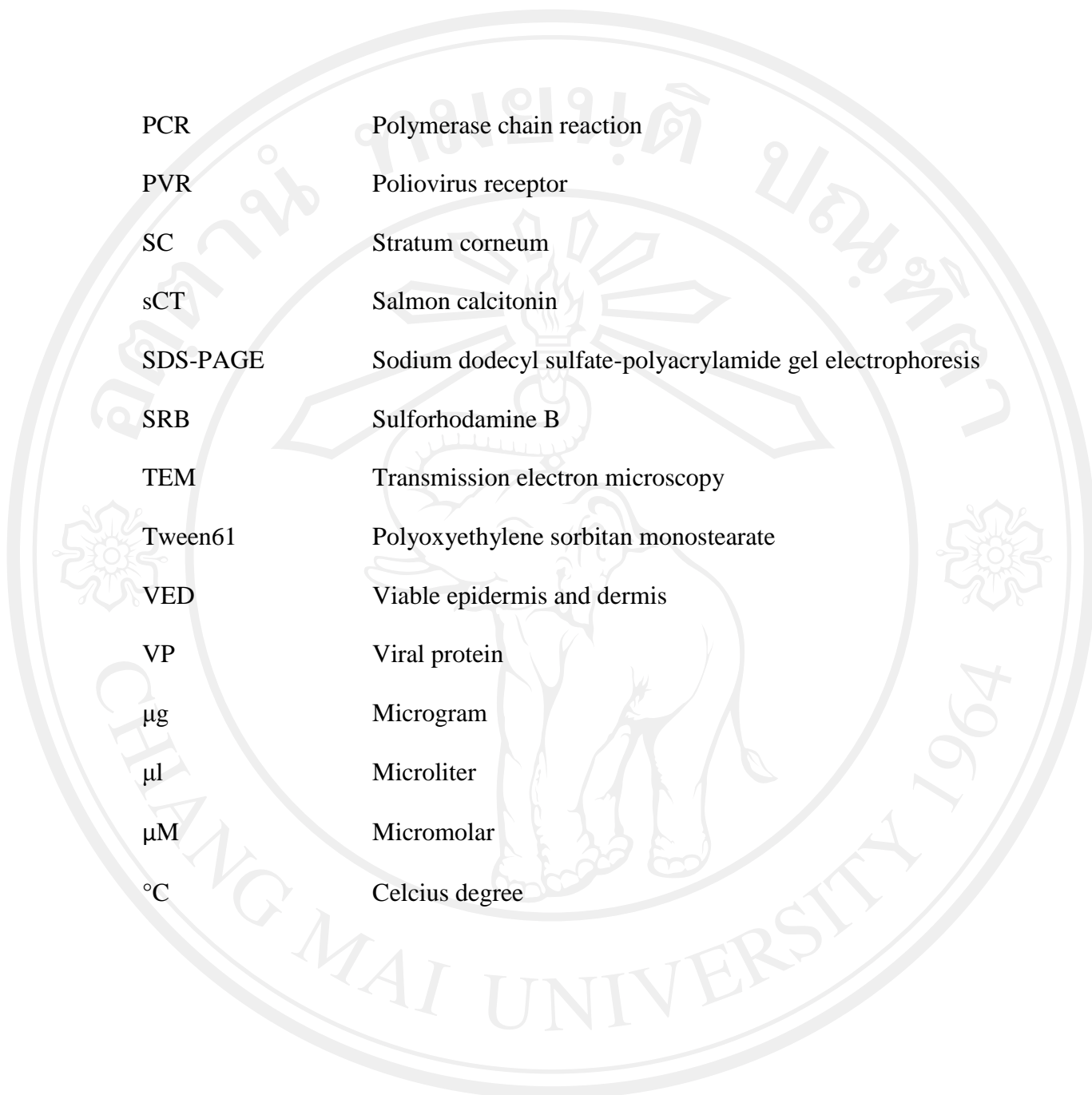
- 36 The negative staining TEM images of (a) blank elastic anionic niosomes (Tween61/CHL/DP/NaC at 1:1:0.02 molar ratio, 1 mol% NaC) (b) Tat-GFP loaded elastic anionic niosomes 158
- 37 Comparison of cellular uptake at various time intervals of GFP, Tat:GFP fusion protein (Tat-GFP) and mixture (Tat/GFP) into HT-29 cells. The folds of Tat/GFP uptake in comparing to Tat-GFP and GFP at 1 hour were labeled above the bar chart. 165
- 38 Transepithelial permeation of GFP, Tat-GFP and Tat/GFP through HT-29 cells. Percentages of protein in lower chamber comparing with the total protein added into each well were presented. The concentration of all samples was equivalent to 2 μ M of GFP. Tat/GFP at 1:1 molar ratio was used. 166
- 39 Cellular uptake (%) of GFP, mixture of GFP, VP1 BC loop (VP) and Tat into the HT-29 (A) and KB cells (B). The concentration of GFP was 1 μ M at all molar ratio. The molar ratio with the highest GFP uptake in each mixture was specified by asterisk and folds of uptake comparing with GFP were labeled. 171

- 40 Agarose gel electrophoresis of poliovirus receptor (PVR, CD155; 349 bp) transcripts amplified by RT-PCR from KB cells (lane 1) and HT-29 cells (lane 2). Lane 3 was the 100 kb DNA ladder. 172
- 41 Differential scanning calorimetry (DSC) thermograms of sCT (A), Tat (B) VP (C), Tat/sCT mixture (D), VP/sCT mixture (E) and VP/Tat/sCT mixture (F) 175
- 42 FT-IR spectra of sCT (A), Tat (B) VP (C), Tat/sCT mixture (D), VP/sCT mixture (E) and VP/Tat/sCT mixture (F) 178
- 43 Relative intracellular calcium (%) after incubation with sCT (fixed concentration 100 pg/ml), Tat (61.22 pg/ml), VP (61.22 pg/ml) and Tat/VP/sCT mixtures at various molar ratios. The direction of particle size increasing was indicated by arrow. 183
- 44 Relative serum calcium level in: **A.** Subcutaneous administration of sCT at various doses of 10, 50, 100, 250 and 500 $\mu\text{g}/\text{kg}$. **B.** Oral administration of sCT, Tat, VP at 32 $\mu\text{g}/\text{kg}$ (3.64 μM) and the mixtures containing sCT equivalent to 50 $\mu\text{g}/\text{kg}$. 185

45	Cumulative amounts ($\mu\text{g}/\text{cm}^2$) and fluxes ($\mu\text{g}/\text{cm}^2\text{hr}$) of sCT of each sample in VED and receiver compartment solution at 1, 3 and 6 hour	189
46	Percentages of sCT (%) detected in each compartment at various time intervals calculated from the initial sCT concentration in the sample (2.5 mg/ml)	190
B.1	Restriction sites of the pWH105-gfpmut2 map	242
B.2	Restriction sites of the pET28a(+) map under T7 promoter	243

ABBREVIATIONS AND SYMBOLS

BSA	Bovine serum albumin
CHL	Cholesterol
CPP	Cell penetrating peptide
DDAB	Dimethyl dioctadecyl ammonium bromide
DMEM	Dulbecco's Modified Eagle's Medium
DP	Dicetyl phosphate
DPPC	L- alpha -dipalmitoyl phosphatidylcholine
DSC	Differential scanning calorimeter
<i>E.coli</i>	<i>Escherichia coli</i>
FBS	Fetal bovine serum
FDEL	Freeze dried empty liposomes
FT-IR	Fourier-transform infrared
HPLC	High performance liquid chromatography
HRP	Horseradish peroxidase
HT-29	Human colon adenocarcinoma
KB	Human mouth epidermal carcinoma
mV	Millivolt
NaC	Sodium cholate
NaDC	Sodium deoxycholate
nm	Nanometer
PBS	Phosphate-buffered saline



PCR	Polymerase chain reaction
PVR	Poliovirus receptor
SC	Stratum corneum
sCT	Salmon calcitonin
SDS-PAGE	Sodium dodecyl sulfate-polyacrylamide gel electrophoresis
SRB	Sulforhodamine B
TEM	Transmission electron microscopy
Tween61	Polyoxyethylene sorbitan monostearate
VED	Viable epidermis and dermis
VP	Viral protein
μg	Microgram
μl	Microliter
μM	Micromolar
$^{\circ}\text{C}$	Celsius degree

ลิขสิทธิ์มหาวิทยาลัยเชียงใหม่

Copyright© by Chiang Mai University
All rights reserved